Surrogate modeling for mechanized tunneling simulations with uncertain data

S. Freitag[1,2)], B. T. Cao[2], J. Ninić[2] and G. Meschke[2]
[1] *Collaborative Research Center Interaction Modeling in Mechanized Tunneling, Ruhr University Bochum, Universitätsstr. 150, 44801, Bochum, Germany; email: steffen.freitag@sd.rub.de*
[2] *Institute for Structural Mechanics, Ruhr University Bochum, Universitätsstr. 150, 44801, Bochum, Germany; email: steffen.freitag@sd.rub.de, ba.cao@rub.de, jelena.ninic@rub.de, guenther.meschke@rub.de*

Abstract. Computational reliability assessment in mechanized tunneling requires realistic numerical models accounting for the uncertainty of geotechnical and tunneling process parameters. For real-time prognoses, surrogate models are in general inevitable to substitute expensive complex numerical simulations. In this paper, different strategies for surrogate modeling in mechanized tunneling simulations are presented. The focus is on surrogate models for reliability analyses with polymorphic uncertain data described by e.g. stochastic numbers, p-boxes, fuzzy stochastic numbers, fuzzy numbers as well as intervals. Beside surrogate models based on Proper Orthogonal Decomposition Method (POD) and Artificial Neural Networks (ANN), a hybrid surrogate model, i.e. a combination of POD and ANN, is presented. Thereby, uncertain time varying surface settlements of several monitoring points are predicted by recurrent neural networks. Based on that, spatially varying surface settlements are evaluated using POD. Utilizing this surrogate model helps to reduce the computation time, when limit states at multiple surface positions are required.

Keywords: surrogate models; Proper Orthogonal Decomposition; Artificial Neural Networks; uncertainty; reliability analysis; mechanized tunneling

1. Introduction

The prediction of tunneling induced surface settlements is important to design and to steer mechanized tunneling processes. A prototype for a process-oriented, three-dimensional, finite element (FE) model for simulations of shield-driven tunnels in soft, water-saturated soil has been proposed by (Kasper and Meschke, 2004) and successfully used for systematic numerical studies of interactions in mechanized tunneling (Kasper and Meschke, 2006). An advanced and flexible software architecture (Nagel et al., 2010) has been developed for this model, which is supplemented with an automatic model generator (Stascheit et al., 2007) allowing a user friendly generation of FE models including all components and their (time-dependent) interactions involved in mechanized tunneling (i.e. fully and partially saturated soft soils, the shield machine steered via hydraulic jacks, the segmented lining, various types of face support, and the tail void grouting).

The soil is modeled as a three or two phase material for partially or fully saturated soils, respectively, see (Nagel and Meschke, 2010). The tunnel boring machine (TBM) is modeled as

a deformable body connected with frictional contact to the soil along the (conical) shield skin. A surface-to-surface contact algorithm using the Augmented Lagrangian Method (Laursen, 2002) is employed allowing a smooth advancement of the machine. The hydraulic jacks are represented by truss elements, which are connected to element nodes of the tunnel lining and connected to the pressure bulkhead of the TBM. To accomplish the desired driving path of the shield, an automated steering algorithm similar to (Kasper and Meschke, 2004) is employed. To ensure stability of the tunnel face due to distortions caused by the excavation process and to reduce ground loss behind the tapered shield, face support pressure and grouting pressures are applied, respectively. The tail void grout is described as a fully saturated two-phase material considering hydration-dependent material properties of the cementitious grouting material as proposed in (Meschke, 1996). This formulation allows for the modelling of infiltration of fluid grout into the surrounding soil. After each TBM advance, the excavation at the cutting face, the tail void grouting and the erection of a new lining ring during standstill are taken into account by deactivation of soil elements at the cutting face, introducing new elements for the grout and the tunnel lining, connecting the jack elements to the new lining elements and computing one or more time steps with updated boundary conditions for the grouting pressure and for the face support pressure.

Concepts for reliability analyses in mechanized tunneling taking epistemic and aleatoric sources of uncertainty into account are presented in (Freitag et al., 2013b). Thereby, stochastic, interval, fuzzy, and imprecise probability approaches are combined within reliability analyses. A corresponding example is presented in (Stascheit et al., 2013).

2. Polymorphic Uncertain Data

Uncertainties of structural parameters (representing structural actions and describing the structural behavior) can be considered by several approaches, e.g. stochastic, interval, fuzzy, or generalized approaches. Due to limited information of input parameters in mechanized tunneling, e.g. parameters describing the local geology and the corresponding soil behavior, polymorphic uncertainty models can be utilized taking epistemic and aleatoric sources of uncertainty into account, see e.g. (Möller and Beer, 2008).

2.1. Stochastic Numbers

Stochastic numbers can be used to quantify aleatoric uncertainty of structural parameters, e.g. for parameters describing the geometry and the mechanical behavior of soil layers. Thereby, spatial and time varying uncertainty can be considered. However, an adequate data base with a sufficiently large number of samples is required to select adequate stochastic models and estimate the corresponding parameters of the probability density functions (pdf) and the corresponding cumulative distribution functions (cdf).

Spatial variability of geological parameters can be considered by random fields taking local correlations into account, see e.g. (Papaioannou et al., 2009) and (Phoon and Kulhawy, 1999). In general, assumptions are required to select a correlation function and to define the corresponding correlation length of random fields.

Stochastic processes can be used to quantify time varying uncertain structural parameters. In mechanized tunneling, parameters describing the excavation process, e.g. excavation rates for several soil types are typical examples where enough information is available to model time varying parameters by means of stochastic processes.

2.2. Intervals and Fuzzy Numbers

Intervals and fuzzy numbers are suitable to quantify parameters with epistemic sources of uncertainty, i.e. if only limited information is available.

Intervals

$$x = [x_l,\ x_u] \tag{1}$$

can be used to quantify uncertain geotechnical parameters by means of lower bounds x_l and upper bounds x_u. In general, the interval bounds are defined based on the experience of experts. In geotechnical engineering and tunneling, intervals are used e.g. in the context of rock mass classifications such as the rock mass rating (RMR) system (Bieniawski, 1989). Within interval analysis lower and upper interval bounds of structural responses are computed. Therefor, interval arithmetic (Moore, 1979), the transformation method (Hanss, 2002), or optimization approaches, see e.g. (Möller et al., 2000), can be utilized. Interval finite element approaches, see e.g. (Muhanna et al., 2007) and (Rao et al., 2011), can be used in structural mechanics. An overview of recent advances in interval FE analysis is given in (Moens and Vandepitte, 2005) and (Moens and Hanss, 2011). A comparative geotechnical analysis using stochastic numbers and intervals has been performed in (Beer et al., 2013).

Fuzzy numbers $\tilde{x}$ can be utilized for uncertainty quantification, if interval information can be assessed by membership functions $\mu(x)$, i.e. the level of membership of each realization x to the set $\tilde{x}$ is described by a number between 0 and 1. Imprecise measurements obtained from monitoring during the tunneling construction can be quantified as fuzzy processes. It is also possible to create fuzzy processes within time discretization of data series, see e.g. (Freitag and Graf, 2011), in order to reduce dense machine parameter information for simulations at a coarser time scale. In structural analysis, fuzzy numbers can be handled as sets of $s = 1, \ldots, S$ intervals

$$x_s = [x_{sl},\ x_{su}]\ , \tag{2}$$

if the membership functions are discretized into α-cuts. For each α-cut s, the lower and upper interval bounds are defined by

$$x_{sl} = \min\left[x \in \mathbb{R} \mid \mu(x) \geq \alpha_s\right] \tag{3}$$

and

$$x_{su} = \max\left[x \in \mathbb{R} \mid \mu(x) \geq \alpha_s\right]\ , \tag{4}$$

respectively. The α-cut representation of fuzzy numbers enables to utilize interval approaches for structural analyses, see e.g. (Muhanna and Mullen, 1999), (Fetz et al., 1999), and (Möller et al., 2000). In (Fetz et al., 1999), fuzzy models are also applied for computations in geotechnical engineering.

2.3. Generalized Uncertainty Models – Probability Boxes and Fuzzy Stochastic Numbers

Imprecise probability concepts can be applied to quantify the variability of uncertain parameters in case of limited statistical information, e.g. small sample sizes for estimation of corresponding stochastic models. The probability box (p-box) approach, see e.g. (Ferson et al., 2003), can be used to define imprecise stochastic numbers by its lower and upper bound cdf. In this case, the probability of each realization is an interval. In general, arbitrary stochastic models, including empirical distributions, can be used for the lower and upper bound cdf. In (Nasekhian and Schweiger, 2011), p-boxes are used within a random set finite element analysis for reliability assessment of tunnel construction according to the New Austrian Tunneling Method.

An alternative is the concept of fuzzy stochastic numbers. In this case, the probability of each realization is a fuzzy number. Fuzzy stochastic numbers can be described by stochastic models with fuzzy model parameters, see (Möller and Beer, 2004), or by sets of p-boxes, see (Freitag et al., 2013a). In (Beer et al., 2013) and (Stascheit et al., 2013), soil parameters are described as fuzzy stochastic numbers within fuzzy stochastic analyses.

3. Surrogate Models

Mechanized tunneling simulations with polymorphic uncertain data are time consuming in general. The computational effort can be prohibitively large within stochastic or fuzzy stochastic analyses, if a large number of realizations is required. Especially to support steering decisions in mechanized tunneling in real-time, surrogate models are required to describe dependencies between uncertain geotechnical and tunneling process parameters and the corresponding uncertain structural responses, e.g. surface settlements. Several approaches for the generation of surrogate models have been developed, see e.g. (Simpson et al., 2001) for an overview. In this paper, it is focused on the development of a new hybrid surrogate model based on Artificial Neural Networks and Proper Orthogonal Decomposition approaches.

3.1. Artificial Neural Networks

Artificial neural networks (ANNs) are widely used in engineering, see e.g. (Adeli, 2001). Often, multilayer perceptrons with feed forward architecture, see (Haykin, 1999), are utilized to learn functional relationships in deterministic data. Applications of neural network based surrogate models replacing deterministic simulation models within stochastic analyses are presented e.g. in (Papadrakakis et al., 1996), (Hurtado, 2002), (Papadrakakis and Lagaros, 2002) and (Most and Bucher, 2007).

In (Ninić et al., 2011) and (Ninić et al., 2013), feed forward neural networks are used to predict surface settlements due to mechanized tunneling. The networks are trained with data obtained from numerical simulations using the process oriented FE model for mechanized tunneling described in Section 1.

For the approximation and prediction of dependencies between structural processes, recurrent neural networks (RNNs) can be used, see e.g. (Freitag et al., 2011). As an extension to feed

forward neural networks, context neurons are added to the hidden and output neurons in order to consider history dependencies in structural processes. RNNs are able to learn dependencies between data series without considering time as additional input parameter. It is possible to capture time-dependent phenomena in data series and predict (extrapolate) further structural responses with RNNs. They can be trained e.g. by modified backpropagation algorithms, see (Freitag et al., 2011), or by means of particle swarm optimization, see (Freitag et al., 2012). In (Stascheit et al., 2013), a RNN surrogate model is utilized within a fuzzy stochastic simulation of a mechanized tunneling process.

3.2. Proper Orthogonal Decomposition

Proper Orthogonal Decomposition (POD) is a powerful method to get a compact representation of data. The purpose of the method is acquired by means of projecting high-dimensional data into a lower-dimensional space. The subspace is spanned by the eigenvectors corresponding to the largest eigenvalues of the sample covariance matrix. Depending on the area of application the method is known under different names, such as Karhunen-Loeve Decomposition (KLD), Principal Component Analysis (PCA) or Singular Value Decomposition (SVD). An overview and short summary of POD method is presented in (Chatterjee, 2000). Up to now, POD has been widely developed and applied for different applications. For inverse analysis of parameter identification processes, a technique that combines POD with Radial Basis Functions (RBF) to produce quick prediction of the system response is presented in (Buljak and Maier, 2011). In (Kahledi et al., 2014), a POD-RBF surrogate model for a mechanized tunneling simulation is used.

3.2.1. *Proper Orthogonal Decomposition and Radial Basis Functions Approximation*

Firstly, a concept of snapshots is introduced, which is a collection of N sampled values of a system output field. One snapshot contains the output field of the system corresponding to a certain realization of input parameters. The outputs are discrete values of the field of interest, like nodal displacements, nodal stress values, internal forces, etc. The collection of M snapshots obtained by numerical simulations generated by changing the input parameters are stored in a rectangular N by M matrix $\mathbf{U}$. The aim of POD is to compute the set of orthonormal vectors (POD basis vectors) $\mathbf{\Phi}$. In general, this can be done by employing SVD technique or solving the eigenvalue problem of the sample covariance matrix $\mathbf{C} = \mathbf{U}^{\mathrm{T}} \cdot \mathbf{U}$. The latter is presented here.

The POD basis can be expressed by a linear transformation of the snapshots $\mathbf{U}$

$$\mathbf{\Phi} = \mathbf{U} \cdot \mathbf{V} \,, \tag{5}$$

where $\mathbf{V}$ is a modal matrix obtained by solving the following eigenvalue problem

$$\mathbf{C} \cdot \mathbf{V} = \mathbf{\Lambda} \cdot \mathbf{V} \,. \tag{6}$$

Here, $\mathbf{\Lambda}$ is a diagonal matrix storing the eigenvalues λ_i of $\mathbf{C}$. The POD vectors are sorted in descending order of corresponding eigenvalues. Having in mind that the eigenvalues of the covariance matrix encode the variability of the data in an orthogonal basis that captures as much of the data's variability as possible in the first few basis functions, it is now easy to construct a low-order

Table I. POD procedure to find the basis vectors capture a desired accuracy

Input: Snapshots matrix $\mathbf{U}$, desired accuracy E
Output: Truncated POD basis vectors $\overline{\mathbf{\Phi}}$
1: Compute covariance matrix $\mathbf{C} = \mathbf{U}^{\mathrm{T}} \cdot \mathbf{U}$
2: Compute eigenvalue decomposition $[\mathbf{\Psi}, \mathbf{\Lambda}] = eig(\mathbf{C})$
3: Set $\mathbf{\Phi}_i = \mathbf{U} \cdot \mathbf{\Psi}_{-,i} / \sqrt{\lambda_i}$
4: Set $\lambda_i = \mathbf{\Lambda}_{ii}$ for $i = 1, ..., M$
5: Define K based on desired accuracy E as following $\sum_{i=1}^{K} \lambda_i / \sum_{i=1}^{M} \lambda_i \geqslant E$
6: **return** truncated POD basis $\overline{\mathbf{\Phi}}$ by taking the first K columns of $\mathbf{\Phi}$

approximation by keeping just the first couple of POD vectors. The truncation of the POD basis is accomplished by deciding a desired accuracy. The resulting POD basis $\overline{\mathbf{\Phi}}$, denoted as *truncated POD basis*, consists of $K << M$ vectors. K is the number of necessary POD basis vectors to capture the desired accuracy. The POD algorithm is summarized in Table I.

Basically, the snapshots matrix $\mathbf{U}$ can be expressed in the new basis by a linear transformation

$$\mathbf{U} = \mathbf{\Phi} \cdot \mathbf{A} \ , \tag{7}$$

where $\mathbf{A}$ represents the amplitude matrix associated with snapshots $\mathbf{U}$. Considering the orthogonality $\mathbf{\Phi}^T \cdot \mathbf{\Phi} = \mathbf{I}$, matrix A can be obtained from

$$\mathbf{A} = \mathbf{\Phi}^T \cdot \mathbf{U} \ . \tag{8}$$

Now $\mathbf{U}$ and a single snapshot of $\mathbf{U}$ can be approximated as

$$\mathbf{U} \approx \overline{\mathbf{\Phi}} \cdot \overline{\mathbf{A}} \tag{9}$$

$$\mathbf{U}_i \approx \overline{\mathbf{\Phi}} \cdot \overline{\mathbf{A}}_i \ , \tag{10}$$

where $\overline{\mathbf{A}}$ and $\overline{\mathbf{A}}_i$ are the *truncated* amplitude matrix and vector, respectively. At this step, $\overline{\mathbf{A}}$ and $\overline{\mathbf{A}}_i$ contains constant values and therefore Eq. (10) represents an approximation only for snapshots generated in the original snapshots matrix $\mathbf{U}$. To pass from this type of a response to a rather continuous one, each amplitude vector is expressed as a nonlinear function of input parameters on which the system depends. Specifically, each amplitude is defined as a linear combination of vector $\mathbf{F}_i = [f_1(\mathbf{z}^i)...f_j(\mathbf{z}^i)...f_M(\mathbf{z}^i)]^T$ being a set of predefined interpolation functions $f_j(\mathbf{z})$ of input parameters $\mathbf{z}$ in the following form

$$\overline{\mathbf{A}}_i = \mathbf{B} \cdot \mathbf{F}_i \ , \tag{11}$$

where $\mathbf{B}$ contains all interpolation coefficients. The choice of $f_j(\mathbf{z})$ can be arbitrary and in this study RBF have been employed as interpolation functions. A description of these functions can be found in (Hardy, 1990). Here, an inverse multiquadric radial function is chosen. This type of RBF function is defined as

$$f_j(\mathbf{z}^i) = f_j(|\mathbf{z}^i - \mathbf{z}^j|) = \frac{1}{\sqrt{|\mathbf{z}^i - \mathbf{z}^j|^2 + r^2}} \ , \tag{12}$$

Table II. POD-RBF procedure to predict output system response from an arbitrary set of input parameters

Input: Snapshots output matrix $\mathbf{U}$, snapshots input matrix $\mathbf{z}$, arbitrary input vector $\mathbf{z}^*$, desired accuracy E
Output: System response vector $\mathbf{U}^*$
1: Compute truncated POD basis $\overline{\mathbf{\Phi}}$ based on E (see Algorithm in Table I)
2: Compute $f_j(\mathbf{z}^i)$ from Eq. (12) with $\mathbf{z}^i = \mathbf{z}^*$ and $i, j = 1, ..., M$
3: Form matrix $\mathbf{F}$ from previous step
4: Compute $\overline{\mathbf{A}} = \overline{\mathbf{\Phi}}^{\mathrm{T}} \cdot \mathbf{U}$
5: Compute $\mathbf{B}$ based on $\mathbf{F}$, $\overline{\mathbf{A}}$
6: Compute $f_j(\mathbf{z}^*)$ from Eq. (12) with $j = 1, ..., M$
7: Form vector $\mathbf{F}^*$ from previous step
8: **return** System response vector $\mathbf{U}^* = \overline{\mathbf{\Phi}} \cdot \mathbf{B} \cdot \mathbf{F}^*$

where r represents smoothing factor and $\mathbf{z}^j$ is a known value of the $\mathbf{z}$ vector. The matrix $\mathbf{F}$ of interpolation functions can be constructed based on all vectors $\mathbf{F}^i$ of input parameters that are used to generate the snapshots. The full form of Eq. (11) is given by

$$\overline{\mathbf{A}} = \mathbf{B} \cdot \mathbf{F} \,, \tag{13}$$

with

$$\overline{\mathbf{A}} = \overline{\mathbf{\Phi}}^{\mathrm{T}} \cdot \mathbf{U} \,. \tag{14}$$

From Eqs. (13) and (14), the coefficient matrix $\mathbf{B}$ is evaluated. Finally, an approximation of the output system response corresponding to an arbitrary set of input parameters can be obtained by

$$\mathbf{U}_i \approx \overline{\mathbf{\Phi}} \cdot \mathbf{B} \cdot \mathbf{F}_i \,. \tag{15}$$

The summary of POD-RBF approach is given in Table II. More details about verification of POD-RBF approach can be found in (Buljak and Maier, 2011).

3.3. Gappy Proper Orthogonal Decomposition

Another extension of POD called Gappy POD (GPOD) has been developed by (Everson and Sirovich, 1995) to reconstruct human face images from incomplete data sets. This approach is based on a combination of basic POD method with linear regression. The basic idea of GPOD is that the POD basis together with gappy data (which are data given at very few of the grid points) are utilized to reconstruct the complete vector for the entire grid. In (Bui-Thanh et al., 2004), this methodology was successfully employed for data reconstruction in the field of aerodynamic. The paper shows a very effective way to reconstruct the flowfields from incomplete aerodynamic data set by using GPOD. The corresponding procedure is described below.

Firstly, the locations of missing data must be identified. A vector $\mathbf{m}$ is introduced to indicate available and missing data. Each element of $\mathbf{m}$ is defined as

$$\begin{aligned} m_i &= 0, \quad \text{for locations of unknown or missing data} \\ m_i &= 1, \quad \text{for locations of known data} \,. \end{aligned} \tag{16}$$

Table III. GPOD procedure to reconstruct the complete solution vector from incomplete solution vector

Input: Snapshots output matrix $\mathbf{U}$, mask vector $\mathbf{m}$, incomplete solution vector $\mathbf{U}^*$, desired accuracy E
Output: Complete solution vector $\mathbf{U}^*$
1: Compute truncated POD basis $\overline{\mathbf{\Phi}}$ based on E (see Algorithm in Table I)
2: Compute $\mathbf{M} = (\overline{\mathbf{\Phi}}^{\mathrm{T}}, \overline{\mathbf{\Phi}})$
3: Compute $\mathbf{R} = (\overline{\mathbf{\Phi}}^{\mathrm{T}}, \mathbf{U}^*)$
4: Compute $\overline{\mathbf{A}}^*$ from $\mathbf{M}$ and $\mathbf{R}$
5: Compute $\mathbf{U}^{**} = \overline{\mathbf{\Phi}} \cdot \overline{\mathbf{A}}^*$
6: **return** Complete solution vector $\mathbf{U}^*$ by replacing missing elements from corresponding elements of $\mathbf{U}^{**}$

Suppose an output system response snapshots set $\mathbf{U}$, where all snapshots are completely known, with the POD basis $\mathbf{\Phi}$ is given. Let $\mathbf{U}^*$ be another solution vector, that has some elements missing, with corresponding mask vector $\mathbf{m}$. The goal here is to reconstruct the complete or "repaired" vector from incomplete vector $\mathbf{U}^*$ with the assumption that $\mathbf{U}^*$ can be characterized with the existing snapshots set $\mathbf{U}$. From Eq. (10), the intermediate repaired vector $\mathbf{U}^{**}$ can be expressed in terms of *truncated* POD basis vectors $\overline{\mathbf{\Phi}}$ as

$$\mathbf{U}^{**} \approx \overline{\mathbf{\Phi}} \cdot \overline{\mathbf{A}}^* \,. \tag{17}$$

The coefficient vector $\overline{\mathbf{A}}^*$ can be computed by minimizing the error $E = ||\mathbf{U}^* - \mathbf{U}^{**}||_n^2$. A solution to this so-called *least squares* or *linear regression* problem is given by a linear system of equations

$$\mathbf{M} \cdot \overline{\mathbf{A}}^* = \mathbf{R} \,, \tag{18}$$

with

$$\begin{aligned} \mathbf{M} &= (\overline{\mathbf{\Phi}}^{\mathrm{T}}, \overline{\mathbf{\Phi}}) \,, \\ \mathbf{R} &= (\overline{\mathbf{\Phi}}^{\mathrm{T}}, \mathbf{U}^*) \,. \end{aligned} \tag{19}$$

Solving Eq. (17) with $\overline{\mathbf{A}}^*$ computed from Eq. (18), the intermediate repaired vector $\mathbf{U}^{**}$ is obtained. Finally, the missing elements in $\mathbf{U}^*$ are replaced by these in $\mathbf{U}^{**}$ and a complete vector of output system responses is obtained. The algorithm of GPOD procedure is shown in Table III.

3.4. Verification of the Gappy Proper Orthogonal Decomposition approach

The proposed GPOD approach is illustrated by means of a verification example from structural analysis, see Figure 1. Here, the deflection of a beam simply supported at both ends with a concentrated load P at point a is investigated. The analytical solution for the deflection line $y(x)$ is given as

$$y(x) \;=\; \frac{P(l-a)x}{6lEI}(l^2 - x^2 - (l-a)^2), \text{ for } 0 < x < a \tag{20}$$

$$y(x) \;=\; \frac{P(l-a)}{6lEI}\left[\frac{l}{l-a}(x-a)^3 + (l^2-(l-a)^2)x - x^3\right],\ \text{for } a<x<l\,. \tag{21}$$

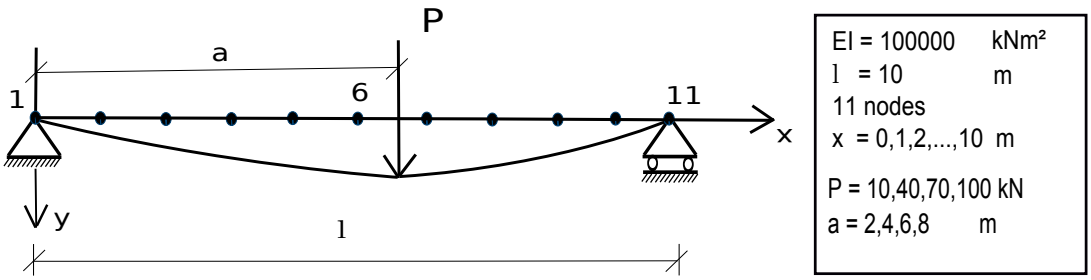

Figure 1. Verification example.

The objective is to predict the deflection of the beam at a number of sections for varying parameters P and a. The structural parameters to set up the example are shown in Figure 1. Here, 16 snapshots are generated based on combining 4 realizations of P and 4 realizations of a. The results of the snapshots computed with Eqs. (20) and (21) are stored in the snapshots matrix $\mathbf{U}$. The snapshots matrix $\mathbf{U}$ consists of 16 columns and 11 rows corresponding to 16 snapshots of the deflections in mm at 11 nodes of the beam, respectively.

$$\mathbf{U} = \begin{bmatrix}
0 & 0 & 0 & 0 & 0 & 0 & 0 & 0 & 0 & 0 & 0 & 0 & 0 & 0 & 0 & 0 \\
0.5 & 1.9 & 3.3 & 4.7 & 0.6 & 2.5 & 4.4 & 6.3 & 0.6 & 2.2 & 3.9 & 5.5 & 0.3 & 1.3 & 2.2 & 3.2 \\
0.9 & 3.4 & 6 & 8.5 & 1.2 & 4.8 & 8.4 & 12 & 1.1 & 4.3 & 7.5 & 10.7 & 0.6 & 2.5 & 4.3 & 6.1 \\
1.1 & 4.4 & 7.7 & 11 & 1.7 & 6.6 & 11.6 & 16.5 & 1.5 & 6 & 10.5 & 15 & 0.9 & 3.5 & 6.1 & 8.7 \\
1.2 & 4.8 & 8.4 & 12 & 1.9 & 7.7 & 13.4 & 19.2 & 1.8 & 7.3 & 12.7 & 18.1 & 1.1 & 4.3 & 7.5 & 10.7 \\
1.2 & 4.7 & 8.3 & 11.8 & 2 & 7.9 & 13.8 & 19.7 & 2 & 7.9 & 13.8 & 19.7 & 1.2 & 4.7 & 8.3 & 11.8 \\
1.1 & 4.3 & 7.5 & 10.7 & 1.8 & 7.3 & 12.7 & 18.1 & 1.9 & 7.7 & 13.4 & 19.2 & 1.2 & 4.8 & 8.4 & 12 \\
0.9 & 3.5 & 6.1 & 8.7 & 1.5 & 6 & 10.5 & 15 & 1.7 & 6.6 & 11.6 & 16.5 & 1.1 & 4.4 & 7.7 & 11 \\
0.6 & 2.5 & 4.3 & 6.1 & 1.1 & 4.3 & 7.5 & 10.7 & 1.2 & 4.8 & 8.4 & 12 & 0.9 & 3.4 & 6 & 8.5 \\
0.3 & 1.3 & 2.2 & 3.2 & 0.6 & 2.2 & 3.9 & 5.5 & 0.6 & 2.5 & 4.4 & 6.3 & 0.5 & 1.9 & 3.3 & 4.7 \\
0 & 0 & 0 & 0 & 0 & 0 & 0 & 0 & 0 & 0 & 0 & 0 & 0 & 0 & 0 & 0
\end{bmatrix} \tag{22}$$

$\mathbf{U}^*$ represents another deflection field corresponding to $P = 125\,\text{kN}$ and $a = 2.5\,\text{m}$. It is assumed, that only 3 values of deflections are known at nodes 2,6 and 10 (i.e. for $x = 1, 5$ and $9\,\text{m}$). The aim is to predict the complete vector $\mathbf{U}^*$ containing the corresponding deflections at all 11 nodes.

Step 1: Perform POD procedure following Algorithm I. *Input*: Snapshots matrix $\mathbf{U}$ (11×16), desired accuracy $E = 99.9$. *Output*: Truncated POD basis vectors $\overline{\mathbf{\Phi}}$ (11×3).

$$\overline{\mathbf{\Phi}} = \begin{bmatrix} 0 & 0 & 0 \\ 0.1 & -0.3 & 0.3 \\ 0.3 & -0.4 & 0.4 \\ 0.4 & -0.4 & 0.1 \\ 0.4 & -0.3 & -0.3 \\ 0.4 & 0 & -0.4 \\ 0.4 & 0.3 & -0.3 \\ 0.4 & 0.4 & 0.1 \\ 0.3 & 0.4 & 0.4 \\ 0.1 & 0.3 & 0.3 \\ 0 & 0 & 0 \end{bmatrix} \tag{23}$$

Step 2: Predict 3 values of deflections at nodes 2,6 and 10 (i.e. $x = 1, 5$ and $9\,\mathrm{m}$). *Input*: Data of 16 snapshots for 3 deflections at selected nodes. *Output*: Deflections of 3 selected nodes.

$$\mathbf{U}^* = \begin{bmatrix} 6.68 \\ 17.9 \\ 4.83 \end{bmatrix} \tag{24}$$

Step 3: Predict 11 values of deflections of 11 nodes of the beam. *Input*: Snapshots matrix $\mathbf{U}$ (11×16), mask vector $\mathbf{m}$, incomplete vector $\mathbf{U}^*$, desired accuracy $E = 99.9$. *Output*: Complete vector $\mathbf{U}^*$.

$$\mathbf{U}^* = \begin{bmatrix} 0.00 \\ \mathbf{6.68} \\ 12.36 \\ 16.20 \\ 18.03 \\ \mathbf{17.90} \\ 16.17 \\ 13.21 \\ 9.34 \\ \mathbf{4.83} \\ 0.00 \end{bmatrix} \qquad \mathbf{U}^{analytical} = \begin{bmatrix} 0.00 \\ \mathbf{6.68} \\ 12.42 \\ 16.32 \\ 18.05 \\ \mathbf{17.90} \\ 16.2 \\ 13.24 \\ 9.35 \\ \mathbf{4.83} \\ 0.00 \end{bmatrix} \tag{25}$$

This result shows a very good agreement with $\mathbf{U}^{analytical}$ obtained from analytical solution following Eqs. (20) and (21). The error is just 0.34% calculated by

$$error = \sqrt{\frac{\sum_{i=1}^{N}(\mathbf{U}_i^{analytical} - \mathbf{U}_i^*)^2}{\sum_{i=1}^{N}(\mathbf{U}_i^{analytical})^2}} \times 100\% \tag{26}$$

4. Hybrid Gappy Proper Orthogonal Decomposition and Recurrent Neural Network Approach

In mechanized tunneling, different limit states are in general defined individually for the different components involved (i.e. the soil, the linings, existing buildings etc.). In order to assess the risk of damage of existing buildings, data of the whole surface displacement field are required. For real-time predictions used to support the TBM steering, it is necessary to extrapolate in time with multiple outputs. The former can be handled by RNN and POD can deal with the latter. A scheme of a new hybrid RNN-GPOD approach for surface settlement predictions in mechanized tunneling is presented in Figure 2.

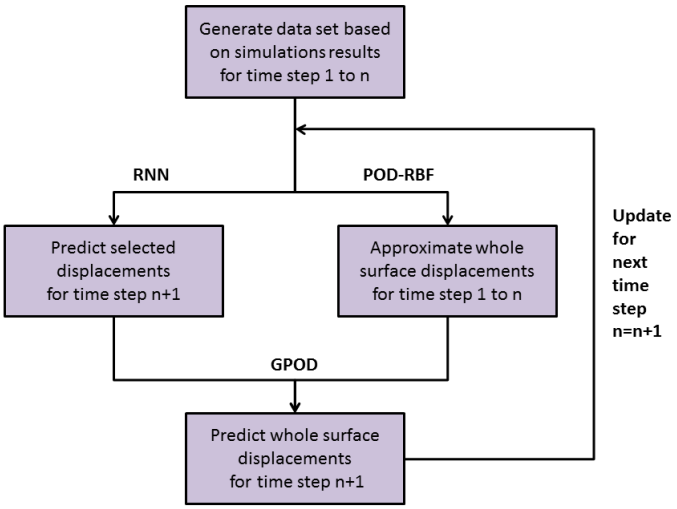

Figure 2. Scheme of hybrid RNN-GPOD approach.

With a numerical model, which is used to simulate a tunneling process from time step 1 to n, a set of data is generated with varying input parameters of the model. Based on these data, the objective is to predict displacements of the whole surface for further tunneling steps corresponding to an arbitrary set of input parameters. Firstly, POD-RBF network is employed to approximate the whole surface displacements from time step 1 to n. Meanwhile, the displacements of several points within the surface field of the next step $n+1$ are predicted by utilizing a RNN. Finally, the GPOD approach is adopted to reproduce the whole displacement field based on a combination of the results from the two previous methods. The predicted results are then included to the available data set and the procedure is repeated for further time steps. The algorithm of the proposed RNN-GPOD approach is shown in Table IV.

Table IV. RNN-GPOD approach to predict whole surface displacements

Offline stage
1: Generate a numerical model representing the current tunneling process from time step 1 to n
2: Define investigated input parameters and the corresponding range of values
3: Run numerical simulations with different input parameters
4: Store the numerical results of displacements of the the whole surface
5: Provide data of several interested points for RNN to train
6: Provide data of whole surface displacements for POD-RBF to train
Online stage
1: Input: an arbitrary set of input parameters
2: Approximate the whole displacements field from time step 1 to n (by POD-RBF)
3: Predict the displacements of several points of next time step $n+1$ (by RNN)
4: Predict the displacements field of next time step $n+1$ (by GPOD)
5: Update the whole displacement field from time step 1 to $n+1$
6: Repeat steps 3 and 4

5. Example

A synthetic example simulating the construction of a tunnel section with 8.5 m diameter and 17 m overburden is generated using the FE model described in Section 1. In Figure 3, the symmetric simulation model with dimensions of 48 m, 85 m and 64 m (in x, y, z directions, respectively) is shown. The length of each excavation step is 1.5 m, i.e the tunnel section consists of 32 steps. The effect of buildings to the surface displacement field is taken into account by applying a distributed load on a part of the ground surface as shown in Figure 4. The tunnel construction process is modeled via a step-by-step procedure consisting of individual phases: soil excavation, applying support pressure, moving shield, applying grouting pressure and lining installation.

The tunnel is completely excavated through the second soil layer of a ground model comprising of three parallel soil layers with different thicknesses and properties, see Figure 3. The groundwater table is constant along the tunnel and at 6 m below the ground surface. A time constant support pressure of 180 kPa is applied at the heading face of the TBM. The grouting pressure P in the tail void is considered as a time varying process parameter. The soil behavior is described by an elastoplastic model using the Drucker-Prager yield criterion with a linear isotropic hardening. Linear elastic behavior is assumed for the shield and tunnel lining. In this study, the elastic modulus E_2 of the second soil layer and the grouting pressure ${}^{[n]}P$ in each excavation step n are chosen as varying parameters. The investigated ranges of these parameters are 40 to 130 MPa for E_2 and 130 to 230 kPa for ${}^{[n]}P$, respectively.

Based on the calculated surface displacements, only an effective surface area of 35 m in y-direction from the tunnel axis is investigated due to the fact, that the displacements of points located further than this distance are almost zero. Figure 4 shows the investigated surface area divided into 99 monitoring points. The z-displacements of these points are considered as outputs of the proposed

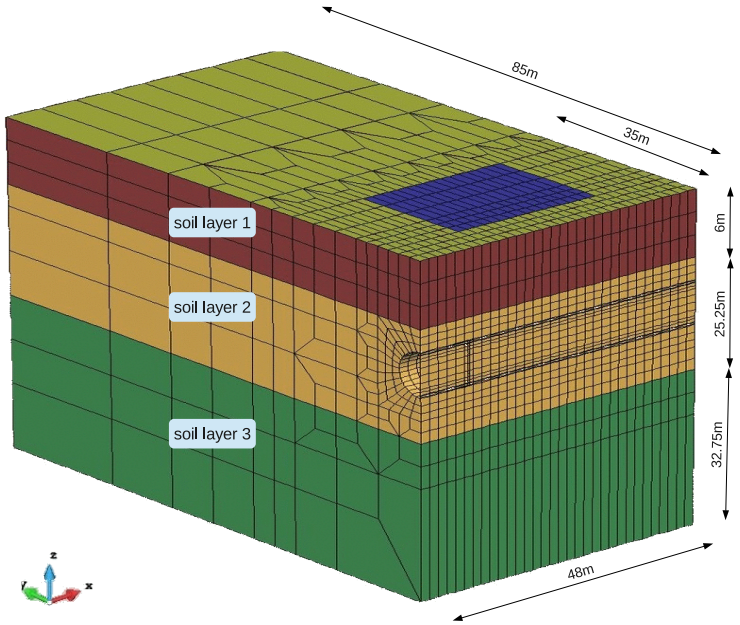

Figure 3. Numerical simulation model of a tunnel section.

hybrid RNN-GPOD approach. Among these 99 points, 7 points are chosen to predict the settlements for future steps using the RNN approach, which are then used to predict the settlements of all 99 points with the GPOD approach. Within the range of the two investigated parameters E_2 and ${}^{[n]}P$, ten particular values for E_2 and six scenarios of time varying ${}^{[n]}P$, see Figure 5, are used to create the surrogate model. In total, 60 FE simulations are carried out.

The data set generated from FE simulation results are divided into training and validation data. Here, 54 training and 6 validation snapshots are used for the GPOD surrogate model. The respective ratio for RNN surrogate model is 30 and 30 snapshots. Each snapshot contains displacement results of 24 time steps. However, for training of the GPOD surrogate model, only results from the first to the 22^{nd} time step are used. Two more time steps (23^{rd} and 24^{th}) are kept for validation. For the RNN surrogate model, data series with 20 time steps are used for network training and data series with 22 time steps are used for validation. The new RNN-GPOD approach is applied to predict (extrapolate) the settlement field containing 99 points for time steps 23 and 24. Because of the length of the used training data series, this objective leads to a two step prognosis for the GPOD part, whereas a four step prognosis is performed within the RNN part. Figures 6 and 7 show predicted results using the described RNN-GPOD approach in comparison with complete FE simulation results (FE) and FE simulation results of the seven surface points only (FE-GPOD) for time steps 23 and 24. The input parameters used to predict both settlement fields are $E_2 = 70\,\text{MPa}$ and ${}^{[n]}P$ according to pressure scenario five, see Figure 5.

In order to consider polymorphic data uncertainty of the soil behavior, interval and stochastic analyses are performed.

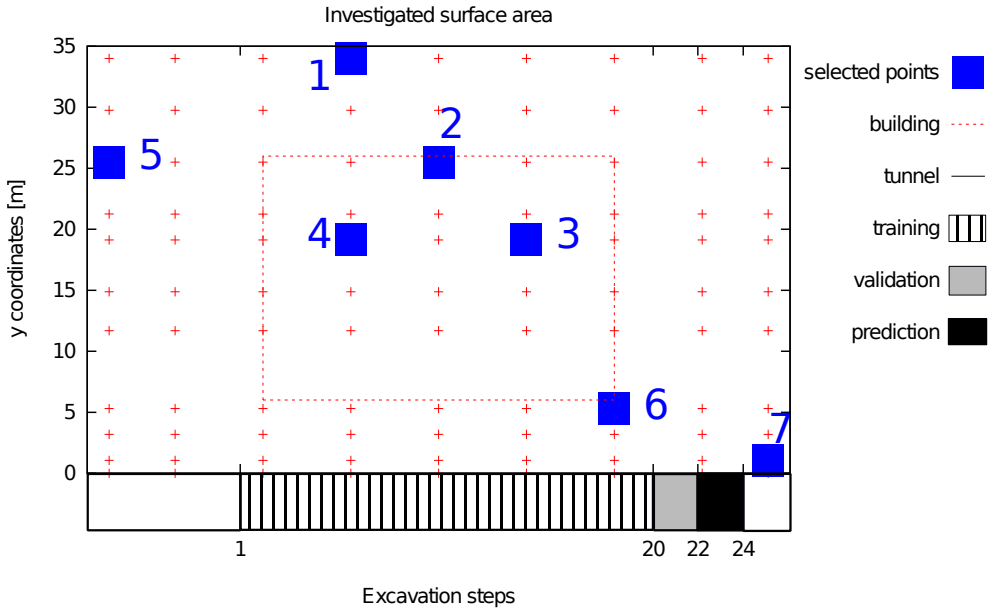

Figure 4. Investigated surface area for settlement predictions.

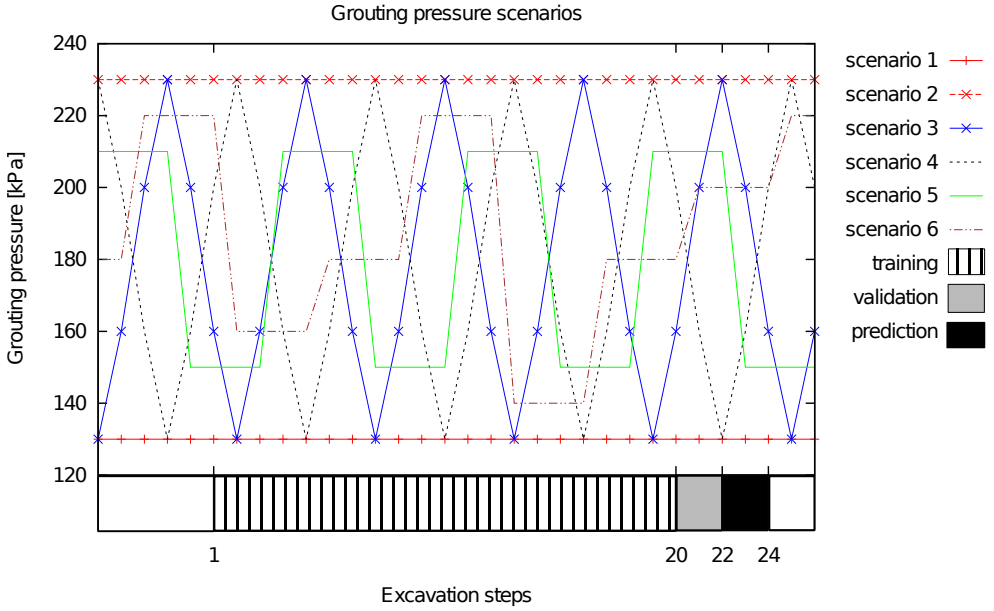

Figure 5. Grouting pressure scenarios.

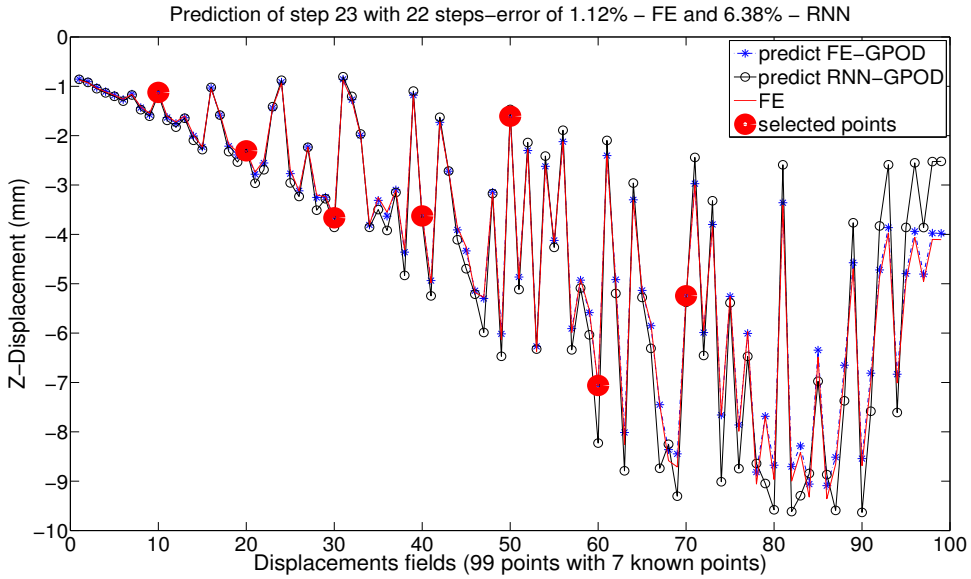

Figure 6. Prediction of displacement field for time step 23.

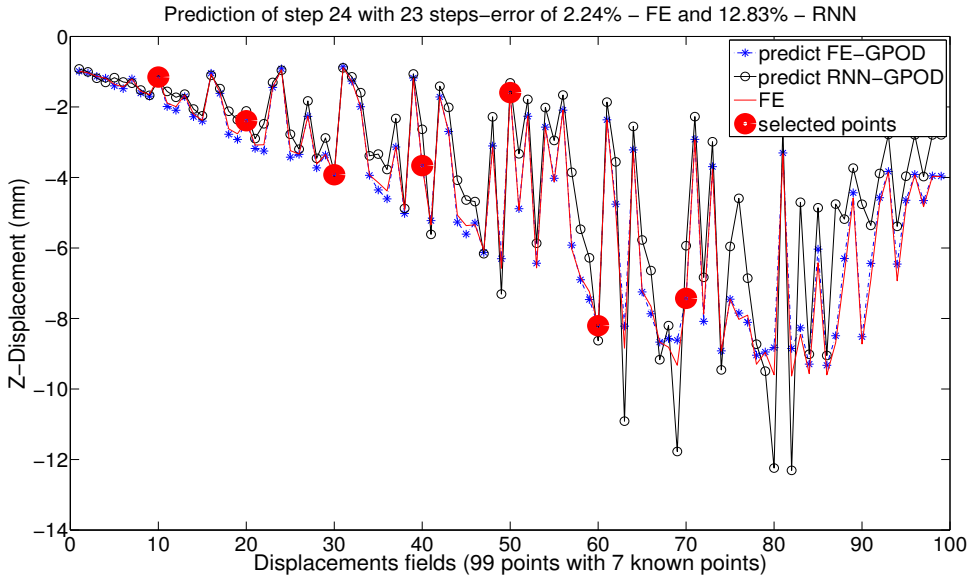

Figure 7. Prediction of displacement field for time step 24.

5.1. Interval Analysis

Assuming the modulus of elasticity E_2 of soil layer two as an interval $E_2 = [74, 86]$ MPa, interval analyses are carried out to compute the tunneling induced time varying settlement field. The interval bounds of each surface node are computed by an optimization approach. In this example, particle swarm optimization (PSO) is employed to identify the minimum and maximum settlements of all surface points during the simulated tunneling process. The number of particles is 20 and the control parameters ($c_1 = c_2 = 1.494$ and $c_3 = 0.729$) are defined according to (Eberhart and Shi, 2001). In Figure 8, the computed interval settlement field is represented by its minimal and maximal bounds.

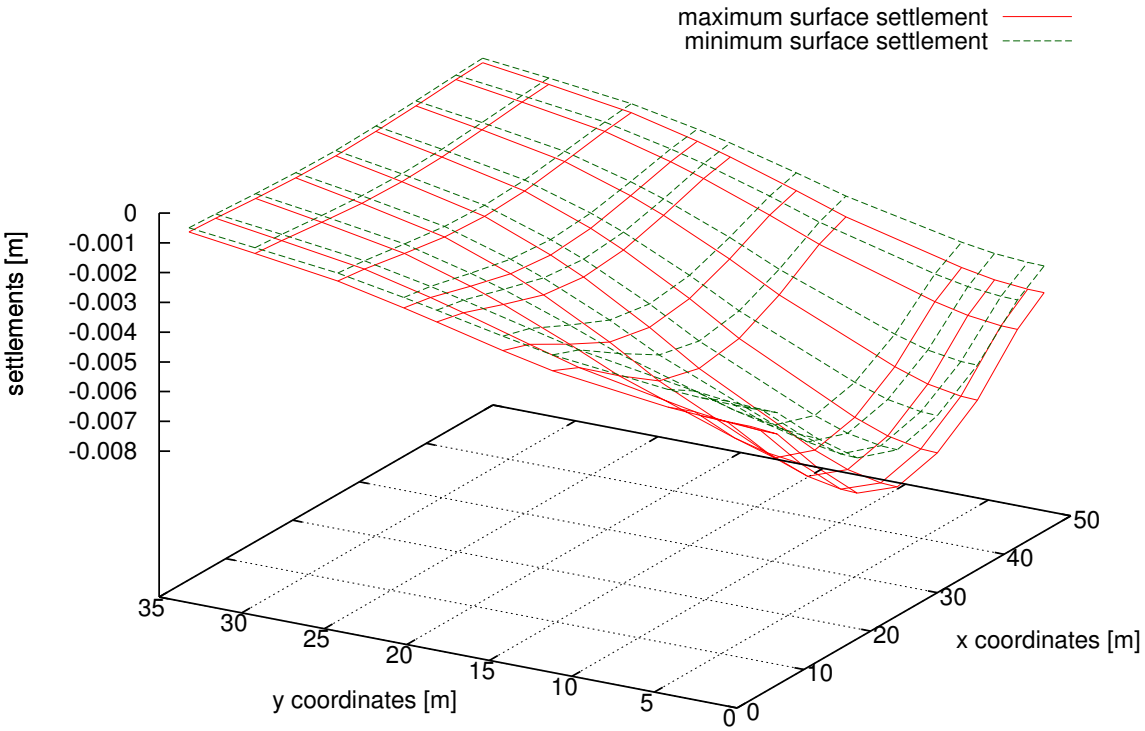

Figure 8. Interval field of tunneling induced surface settlements with $E_2 = [74, 86]$ MPa.

Table V. Different scenarios of changing grouting pressures for time step 23 and time step 24.

scenario	1	2	3	4
grouting pressure of step 23 (kPa)	140	170	200	215
grouting pressure of step 24 (kPa)	140	170	200	215

5.2. Stochastic Analysis

For reliability analyses, the modulus of elasticity E_2 of soil layer two is assumed as a stochastic number with logistic distribution. Its cumulative distribution function (cdf) is defined as

$$F(E_2) = \frac{1}{1 + e^{-\left(\frac{E_2 - a}{b}\right)}} \tag{27}$$

with parameters $a = 80\,\text{MPa}$ (mean value) and $b = 3\,\text{MPa}$, which results in a variance of $29.61\,\text{MPa}^2$. The grouting pressure ${}^{[n]}P$ is considered as a deterministic process according to pressure scenario six, see Figure 5. In order to investigate the effect of changing grouting pressure to the failure probability P_f, several cases of changing grouting pressures for the next two time steps 23 and 24 are considered as given in Table V and Figure 9.

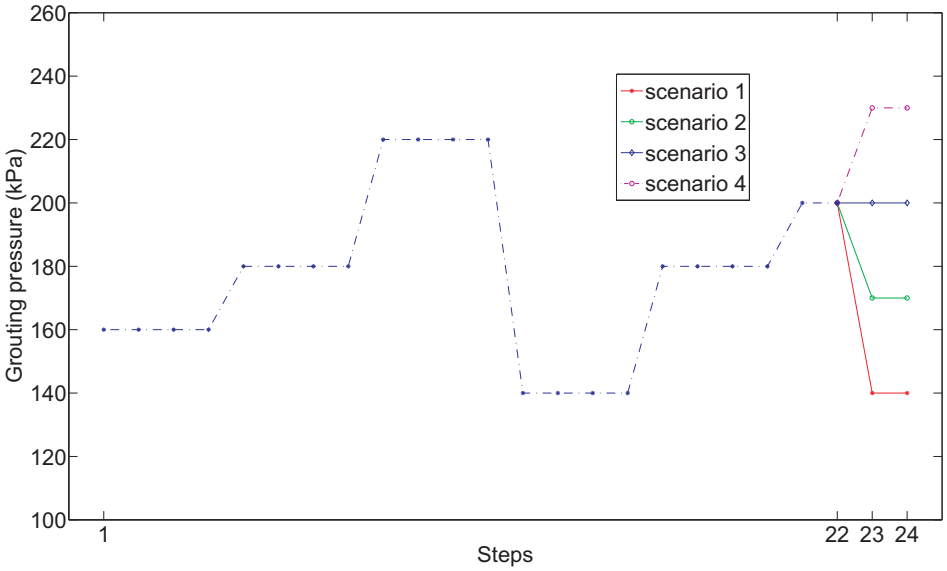

Figure 9. Different scenarios of changing grouting pressures for time step 23 and time step 24.

Failure is defined as an exceeding of the limit state at least for one of the 99 predicted surface settlements. In this example, a limit state of 10 mm is chosen. Figure 10 depicts the failure probabilities computed based on Monte Carlo simulation of the two following time steps 23 and 24 for the four possible grouting pressure cases according to Figure 9.

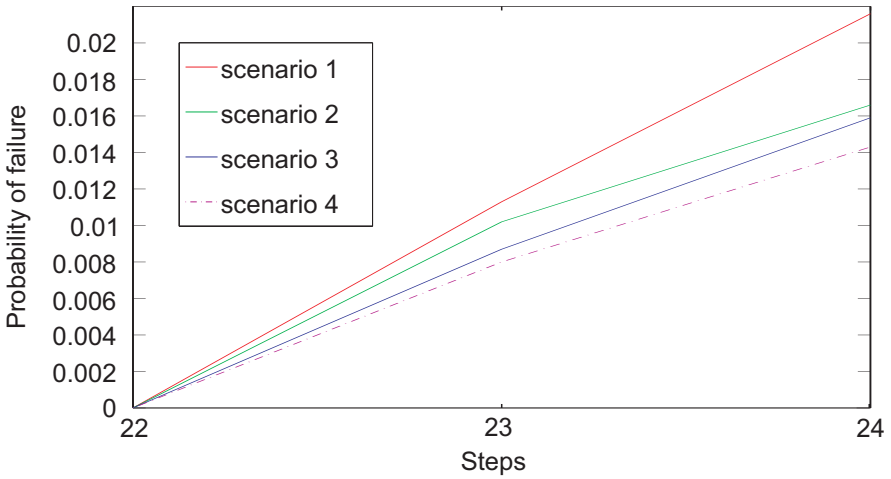

Figure 10. Failure probabilities of time steps 23 and 24 for the grouting pressure scenarios according to Figure 9.

6. Conclusion

A new hybrid surrogate modeling strategy combining POD and ANN approaches has been developed. It is applied for the prediction of spatial and time varying dependencies of structural parameters within mechanized tunneling simulations. RNNs are used to extrapolate surface settlements at selected positions in time and GPOD is applied to construct the corresponding surface settlement fields for varying geotechnical and tunneling process parameters. The applicability is demonstrated within interval and stochastic reliability analyses.

In further works, it will be focused on real-time reliability analyses in mechanized tunneling to support steering decisions, e.g. predict ranges of possible grouting pressures for further tunneling steps. Monitoring data will be implemented to adaptively update the surrogate models.

Acknowledgements

Financial support was provided by the German Science Foundation (DFG) in the framework of project C1 of the Collaborative Research Center SFB 837 "Interaction Modeling in Mechanized Tunneling". This support is gratefully acknowledged.

References

Adeli, H. Neural Networks in Civil Engineering: 1989-2000. *Computer-Aided Civil and Infrastructure Engineering*, 16:126–142, 2001.

Beer, M., Y. Zhang, S. T. Quek and K. K. Phoon. Reliability analysis with scarce information: Comparing alternative approaches in a geotechnical engineering context. *Structural Safety*, 41:1–10, 2013.

Bieniawski, Z. T. *Engineering Rock Mass Classifications.* Wiley, New York, 1989.

Bui-Thanh, T., K. Damodaran and K. Willcox. Aerodynamic Data Reconstruction and Inverse Design using Proper Orthogonal Decomposition. *The American Institute of Aeronautics and Astronautics (AIAA)*, 42:1505–1516, 2011.

Buljak, V. and G. Maier. Proper Orthogonal Decomposition and Radial Basis Functions in Material Characterization Based on Instrumented Indentation. *Engineering Structures*, 33:492–501, 2011.

Chatterjee, A. An Introduction to the Proper Orthogonal Decomposition. *Current Science*, 78:808–817, 2000.

Eberhart, R. C. and Y. Shi. Particle Swarm Optimization: Developments, Applications and Resources. In: *Proceedings of the 2001 IEEE Congress on Evolutionary Computation*, Seoul, 2001.

Everson, R. and L. Sirovich. Karhunen-Loeve Procedure for Gappy Data. *Journal of the Optical Society of America A: Optics, Image Science and Vision*, 12(8):1657–1664, 1995.

Ferson, S., V. Kreinovich, L. Ginzburg, D. S. Myers and K. Sentz. *Constructing probability boxes and Dempster-Shafer structures*. Tech. Rep. SAND2002-4015, Sandia National Laboratories, 2003.

Fetz, T., M. Oberguggenberger, J. Jäger, D. Köll, G. Krenn, H. Lessmann and R. F. Stark. Fuzzy Models in Geotechnical Engineering and Construction Management. *Computer-Aided Civil and Infrastructure Engineering*, 14:93–106, 1999.

Freitag, S. and W. Graf. FE Analysis of Structures with Uncertain Model-Free Material Descriptions. In: *Proceedings of the ASME 2011 International Mechanical Engineering Congress and Exposition (IMECE2011)*, Volume 9, Denver, 831–839, 2011.

Freitag, S., W. Graf, and M. Kaliske. Recurrent Neural Networks for Fuzzy Data. *Integrated Computer-Aided Engineering*, 18(3):265–280, 2011.

Freitag, S., R. L. Muhanna and W. Graf. Interval Monte Carlo simulation with neural network-based surrogate models. In: G. Deodatis, B. R. Ellingwood, D. M. Frangopol (eds.) *Safety, Reliability, Risk and Life-Cycle Performance of Structures and Infrastructures, Proceedings of 11th International Conference on Structural Safety and Reliability (ICOSSAR 2013)*, New York, Taylor and Francis, London, 431–438, 2013.

Freitag, S., R. L. Muhanna and W. Graf. A Particle Swarm Optimization Approach for Training Artificial Neural Networks with Uncertain Data. In: M. Vořechovský, V. Sadílek, S. Seitl, V. Veselý, R. L. Muhanna, R. L. Mullen (eds.) *Proceedings of the 5th International Conference on Reliable Engineering Computing (REC 2012)*, Brno, 2012.

Freitag, S., M. Beer, K. K. Phoon, J. Stascheit, J. Ninić, B. T. Cao and G. Meschke. Concepts for Reliability Analyses in Mechanised Tunnelling – Part 1: Theory. In: G. Meschke, J. Eberhardsteiner, T. Schanz, K. Soga and M. Thewes (eds.) *Proceedings of the Third International Conference on Computational Methods in Tunnelling and Subsurface Engineering (EURO:TUN 2013)*, Bochum, Aedificatio Publishers, Freiburg, 791–799, 2013.

Hanss, M. The transformation method for the simulation and analysis of systems with uncertain parameters. *Fuzzy Sets and Systems*, 130(3):277–289, 2002.

Hardy, R. L. Theory and Applications of the Multiquadric-biharmonic Method: 20 Years of Discovery 1968-1988. *Computers & Mathematics with Applications*, 19(8-9):163–208, 1990.

Haykin, S. *Neural Networks – A Comprehensive Foundation*. Prentice-Hall, Upper Saddle River, 1999.

Hurtado, J. E. Analysis of one-dimensional stochastic finite elements using neural networks. *Probabilistic Engineering Mechanics*, 17:35–44, 2002.

Khaledi, K., T. Schanz and S. Miro. Application of Metamodelling Techniques for Mechanized Tunnel Simulation. *Journal of Theoretical and Applied Mechanics*, 44(1):45–54, 2014.

Kasper, T. and G. Meschke. A 3D Finite Element Simulation Model for TBM Tunnelling in Soft Ground. *International Journal for Numerical and Analytical Methods in Geomechanics*, 28:1441–1460, 2004.

Kasper, T. and G. Meschke. A Numerical Study on the Effect of Soil and Grout Material Properties and Cover Depth in Shield Tunnelling. *Computers & Geotechnics*, 33(4-5):234–247, 2006.

Laursen, T. *Computational Contact and Impact Mechanics*. Springer, Berlin-Heidelberg, 2002.

Meschke, G. Consideration of Aging of Shotcrete in the Context of a 3D Viscoplastic Material Model. *International Journal for Numerical Methods in Engineering*, 39:3123–3143, 1996.

Moens, D. and M. Hanss. Non-probabilistic finite element analysis for parametric uncertainty treatment in applied mechanics: Recent advances. *Finite Element Analysis and Design*, 47:4–16, 2011.

Moens, D. and D. Vandepitte. A survey of non-probabilistic uncertainty treatment in finite element analysis. *Computer Methods in Applied Mechanics and Engineering*, 194:1527–1555, 2005.

Möller, B. and M. Beer. *Fuzzy Randomness – Uncertainty in Civil Engineering and Computational Mechanics*. Springer, Berlin, 2004.

Möller, B. and M. Beer. Engineering computation under uncertainty – Capabilities of non-traditional models. *Computers and Structures*, 86(10):1024–1041, 2008.

Möller, B., W. Graf, and M. Beer. Fuzzy structural analysis using α-level optimization. *Computational Mechanics*, 26(6):547–565, 2000.

Moore, R. E. *Methods and Applications of Interval Analysis*. Studies in Applied Mathematics, Vol. 2, SIAM, Philadelphia, 1979.

Most, T. and C. Bucher. Probabilistic analysis of concrete cracking using neural networks and random fields, *Probabilistic Engineering Mechanics*, 22:219–229, 2007.

Muhanna, R. L. and R. L. Mullen. Formulation of Fuzzy Finite-Element Methods for Solid Mechanics Problems. *Computer-Aided Civil and Infrastructure Engineering*, 14:107–117, 1999.

Muhanna, R. L., H. Zhang, and R. L. Mullen. Interval Finite Elements as a Basis for Generalized Models of Uncertainty in Engineering. *Reliable Computing*, 13(2):173–194, 2007.

Nagel, F. and G. Meschke. An Elasto-plastic Three Phase Model for Partially Saturated Soil for the Finite Element Simulation of Compressed Air Support in Tunnelling. *International Journal for Numerical and Analytical Methods in Geomechanics*, 34:605–625, 2010.

Nagel, F., J. Stascheit and G. Meschke. Process-oriented Numerical Simulation of Shield Tunneling in Soft Soils. *Geomechanics and Tunnelling*, 3(3):268–282, 2010.

Nasekhian A. and H. F. Schweiger. Random set finite element method application to tunnelling. *International Journal for Reliability and Safety*, 5(3/4):299–319, 2011.

Ninić, J., J. Stascheit and G. Meschke. Prediction of Tunnelling Induced Settlements using Simulation-Based Artificial Neural Networks. In: Y. Tsompanakis and B. H. V. Topping (eds.) *Proceedings of the 2nd International Conference on Soft Computing Technology in Civil, Structural and Environmental Engineering*, paper 26, Civil-Comp Press, Stirlingshire, 2011.

Ninić, J., J. Stascheit and G. Meschke. Simulation-based Steering for Mechanized Tunneling Using an ANN-PSO-Based Meta-Model. In: Y. Tsompanakis (ed.) *Proceedings of the 3rd International Conference on Soft Computing Technology in Civil, Structural and Environmental Engineering*, paper 5, Civil-Comp Press, Stirlingshire, 2013.

Papadrakakis, M. and N. D. Lagaros. Reliability-based structural optimization using neural networks and Monte Carlo simulation. *Computer Methods in Applied Mechanics and Engineering*, 191, 3491–3507, 2002.

Papadrakakis, M., V. Papadopoulos, N. D. Lagaros. Structural reliability analysis of elastic-plastic structures using neural networks and Monte Carlo simulation. *Computer Methods in Applied Mechanics and Engineering*, 136, 145–163, 1996.

Papaioannou, I., H. Heidkamp, A. Düster, E. Rank and C. Katz. Random Field Reliability Analysis as a Means for Risk Assessment in Tunnelling. In: G. Meschke, G. Beer, J. Eberhardsteiner, D. Hartmann and M. Thewes (eds.) *Proceedings of the Second International Conference on Computational Methods in Tunnelling (EURO:TUN 2009)*, Bochum, Aedificatio Publishers, Freiburg, 585–592, 2009.

Phoon, K. K. and F. H. Kulhawy. Characterization of geotechnical variability. *Canadian Geotechnical Journal*, 36:612–624, 1999.

Rao, M. V. R., R. L. Mullen, and R. L. Muhanna. A new interval finite element formulation with the same accuracy in primary and derived variables. *International Journal for Reliability and Safety*, 5(3/4):336–357, 2011.

Simpson, T. W., J. D. Peplinski, P. N. Koch and J. K. Allen. Metamodels for computer-based engineering design: survey and recommendations. *Engineering with Computers*, 17:129–150, 2001.

Stascheit, J., S. Freitag, M. Beer, K. K. Phoon, J. Ninić, B. T. Cao and G. Meschke. Concepts for Reliability Analyses in Mechanised Tunnelling – Part 2: Application. In: G. Meschke, J. Eberhardsteiner, T. Schanz, K. Soga and M. Thewes (eds.) *Proceedings of the Third International Conference on Computational Methods in Tunnelling and Subsurface Engineering (EURO:TUN 2013)*, Bochum, Aedificatio Publishers, Freiburg, 801–811, 2013.

Stascheit, J., F. Nagel, G. Meschke, M. Stavropoulou and G. Exadaktylos An Automatic Modeller for Finite Element Simulations of Shield Tunnelling. In: J. Eberhardsteiner and G. Beer and C. Hellmich and H.A. Mang and G. Meschke and W. Schubert, editors, *Proceedings of Computational Modelling in Tunnelling (EURO:TUN 2007)*, Vienna, 2007.